Journal of Solid Mechanics Vol. 11, No. 2 (2019) pp. 297-310
DOI: 10.22034/JSM.2019.665909

An Approximate Solution of Functionally Graded Timoshenko Beam Using B-Spline Collocation Method

D. Mahapatra [1], Sh. Sanyal [2], Sh. Bhowmick [2,*]

[1] *BRSMCAET, IGKV, Mungeli, India*
[2] *Department of Mechanical Engineering, NIT Raipur, India*

Received 13 February 2019; accepted 2 April 2019

ABSTRACT

Collocation methods are popular in providing numerical approximations to complicated governing equations owing to their simplicity in implementation. However, point collocation methods have limitations regarding accuracy and have been modified upon with the application of B-spline approximations. The present study reports the stress and deformation behavior of shear deformable functionally graded cantilever beam using B-spline collocation technique. The material grading is along the beam height and varies according to power law. Poisson's ratio is assumed to be a constant. The equations are derived using virtual work principle in the framework of Timoshenko beams to obtain a unified formulation for such beams. A sixth order basis function is used for approximation and collocation points are generated using Greville abscissa. Deformation and stresses; bending (axial) stresses and transverse (shear) stresses, and position of neutral axis are studied for a wide range of power law index values. The results are reported along the beam cross-section and beam length.

Keywords : Functionally graded beams; B-spline collocation; Timoshenko beams; Power law index.

1 INTRODUCTION

SINCE mid-1980s, with the advent of Functionally Graded Materials (FGMs), we are witnessing a new era in the field of material technology. FGMs, belongs to a class of advanced materials which have continuous variation in properties along a desired direction and in desired fashion. In such materials the composition (volume of constituents) and hence the structure gradually change over the volume, resulting in corresponding change in the properties of the material that is different from either of the parent material. Functionally graded material hence eliminates the sharp interfaces existing in composite materials/ structures where failure is usually initiated. Due to their customized behavior, FGMs may have very wide applications. If their manufacturing cost is reduced by improving the processes, then it may revolutionize the design processes as a whole. A thorough overview about

*Corresponding author. Tel.: +91 9575955040.
E-mail address: sbhowmick.mech@nitrr.ac.in (Sh. Bhowmick).

FGMs, their manufacturing techniques, modeling and design and applications can be referred in [1-5]. In [6] an exhaustive review on the modeling and analysis of functionally graded materials and their applications has been presented. Although considerable research on the functionally graded materials has been reported since their conceptualization, most of the work in the area of functionally graded structures (beams and plates) has been done only in last decade. Reddy and Chin [7] and Reddy [8] have studied and presented for the first time the modeling of FG plates in the framework of shear deformable theory considering the nonlinearities due to large deflection along with the variation in material properties across the thickness. Shankar [9] studied the behavior of FG Euler-Bernoulli beam using elasticity approach and is considered as the most fundamental work in this realm of FG beams. In this work an exponential variation of modulus of elasticity across the thickness is considered, keeping Poisson's ratio constant; the variations in stress and displacements are monitored and the behavior of slender and stubby beams under different loading conditions are compared. In [10] Shankar extended his work to include a temperature gradient across the width of beam, keeping material property variation only dependent on position and independent of temperature; and for the same problem, the author in [11], used the method of Fourier analysis combined with Galerkin's method for solution. Chakraborty et al [12] have developed a new beam element that can be applied to a bi-material shear deformable beam with functionally graded intermediate layer and hence to determine its mechanical response to static and dynamic loads in a thermal environment. Static and vibration analysis using higher order deformation theory for FG beams has been reported in references [13, 15-19]. The approaches to solutions in [13-14, 16-19] are various analytical techniques while computational technique was approached in [15]. In [19], Guinta et al have formulated a unified formulation using a generic N-order approximation for displacement variables of the cross-section and applied the theory to FG beams. The effect of geometric nonlinearity in the form of von Karman relations in the displacement terms has been accounted in [20-22]. Due to the variation in material properties across the cross-section, neutral axis does not coincide with the centre of gravity of the cross-section. The variation of the position of neutral axis with material gradation has been dealt in [22, 23]. An analysis for the FG beam resting on Winkler's foundation and the solution using finite element technique has been reported in [24-25]. Li [26] reported a unique unified formulation for FG Timoshenko beam by reducing the three differential equations of displacement variables into a single fourth order equation. Effect of rotary inertia and shear deformation has been included and the entire formulation may be analytically reduced to Rayleigh and Euler-Bernoulli beam after neglecting a few terms. In recent years B-spline collocation technique is increasingly being used to find solutions to structural problems also. B-splines are widely accepted standards owing to their flexibility and computational efficiency. The collocation technique is quite simpler as compared to Finite Element Method and easy to apply to many problems involving differential equations. A comparative study between the B-spline collocation technique, Finite Element and Finite difference techniques for a two-parameter singularly perturbed boundary value problem has been reported in [27]; the method of B-spline collocation gives better approximation and convergence than the other two techniques. As a thumb rule we may presume that B-spline collocation may be preferred for comparatively simpler geometries like beams/ plates. The technique has been used successfully in fluid flow and one dimensional heat/ mass transfer [28] and also conduction radiation problem [29]. In 1995, Bert et al [30] have applied the method of spline collocation to find approximate solution in statics of beams and plates. Sun et al [31] have reported the application of B-spline collocation to problems of linear elasticity using orthogonal cubic B-spline functions. Vibration analysis of non-uniform beams supported on elastic foundation and of pre-twisted beams using spline collocation with uniform knot span has been carried out by Hsu [32, 33]. The effect of non-uniform knot span in the spline collocation procedure applied to a structural problem has been studied by Wu et al [34]; the author has utilized the concept of Radial Spline functions which includes the knot spacing as a variable, applied the same to beam problems and showed that non-uniform knot spacing gives a better approximation. Multiplicity of the knots may be an additional parameter in the analysis as it reduces the continuity of the spline at the knots. The effect of multiple knots in a structural problem is considered by Provatidis [35] through finite element analysis using cubic B-spline shape functions. Recently, Isogeometric (IG) analysis [36] (using NURBS, which is a refined formulation of B-splines, as shape functions) is increasingly attracting researchers for finding approximate solutions to complex problems. Auricchio et al [37] have reported the applications of IG collocation technique and applied it to theoretical analysis of many mathematical problems. Reali [38] has applied for the first time IG collocation to slender beams and plates and have illustrated the inherent potential of the method. Patlashenko et al [39] have applied the cubic B-spline collocation technique to study the behavior of panels subjected to mechanical and thermal loading. In [40] Patlashenko extended his work to nonlinear analysis of laminated panels using two dimensional spline collocation method. Mizusawa et al [41, 42] have used the concept of spline finite strip method to study the vibration characteristics of cross-ply and thick laminated cylindrical panes. Akhras et al [43] have applied the spline finite strip method to investigate the stability and vibration behavior of piezoelectric composite plates while Loja et al [44] have applied the B-spline finite strip technique to study the static and dynamic behavior of FG sandwiched plates

with piezoelectric skins. In a recent paper, Provaditis [45] has used the B-spline collocation technique to obtain the natural frequencies of thin plates in bending. The results in [45] report the effectiveness of B-spline collocation technique over the cubic B-spline Galerkin-Ritz formulation.

In this paper B-spline collocation technique using sixth order b-spline shape functions is used for finding approximate solutions to the governing differential equations for static analysis of functionally graded shear deformable beam problem.

2 FORMULATION

A functionally graded cantilever beam of length 'L', rectangular dimensions of width 'b' and height 'h', having three dimensional Cartesian coordinate system as shown in Fig. 1 and material property gradation across the cross-section is considered for static analysis. The boundary conditions for a cantilever beam are

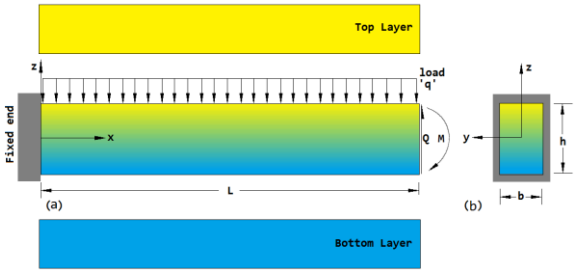

Fig.1
Schematic diagram of FG beam and it coordinate system (a) Front view (b) Side view.

$$\left.\begin{aligned} &\phi(0)=0; w(0)=0; \\ &M_x(L)=0; V_x(L)=0 \end{aligned}\right\} \tag{1}$$

The modulus of elasticity follows power law distribution across the height of the beam (Fig. 2) and is given by

$$E(z)=E_b+(E_t-E_b).\left(\frac{z}{h}+\frac{1}{2}\right)^{\beta} \tag{2}$$

The subscripts 'b' and 't' refers bottom and top fiber respectively and 'β' is the power law index. In the present work Poisson's ratio is assumed to be a constant. As the materials considered in the present case resemble in properties and the variation of Poisson's ratio between them is minimal, hence the assumption of invariable Poisson's ratio is reasonable in the present case. However to generalize the idea to wider arena for considering materials that contrast in properties, the variation of Poisson's ratio ($\mu(z)$, power law depth dependent in present case) can be easily be incorporated in the governing equations. The effect of variation of Poisson's ratio will be seen in rigidity modulus and shear correction factors as shown below

$$G(z)=\frac{E(z)}{2.(1+\mu(z))} \qquad k(z)=\frac{5(1+\mu(z))}{(6+5\mu(z))} \tag{3}$$

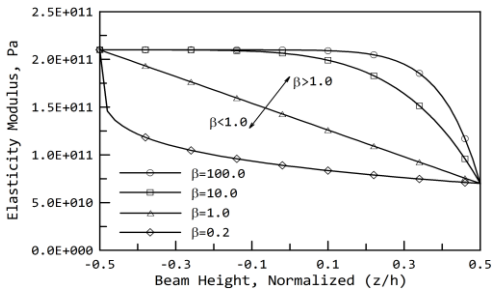

Fig.2
Variation of Modulus of Elasticity across the cross-section with power law index, β.

The above beam is considered to be Timoshenko beam i.e. the effect of shear deformation will be accounted for the displacement variables; loading and corresponding deflection is constrained in the *x*-*z* plane. Let '*u*', '*w*' and 'ϕ' represent the axial and transverse deflection and rotation of the cross-section at the mid-plane respectively. A subscript '0' with the variable (e.g. u_0) will account for the corresponding variable value at mid-plane. The transverse deflection '*w*' and the shear deformation 'γ' are assumed to be functions of '*x*' and are uniform for a cross-section. Based on Timoshenko beam theory:

$$u(x,z) = u_0(x) + z\,\phi(x) \tag{4}$$

$$\epsilon_{xx} = \frac{\partial u}{\partial x} = \frac{\partial u_0}{\partial x} + z\,\frac{\partial \phi}{\partial x} \tag{5}$$

$$\gamma_{xz} = \phi + \frac{\partial w}{\partial x} \tag{6}$$

Virtual work principle states that the variation in strain energy is equal to the work done by the load to cause an infinitesimal deflection of beam i.e.

$$\delta U = \int_0^L \iint (\sigma_{xx}.\delta\epsilon_{xx} + \tau_{xz}.\delta\gamma_{xz}).dx.dA + \int_0^L q.\delta w.dx = 0 \tag{7}$$

$$\sigma_{xx} = E(z).\epsilon_{xx} \tag{8}$$

$$\tau_{xz} = k.G(z).\gamma_{xz} \tag{9}$$

$$dA = b.dz \tag{10}$$

$$\delta U = \int_0^L \iint \{(E(z).\epsilon_{xx}.\delta\epsilon_{xx} + G(z).\gamma_{xz}.\delta\gamma_{xz})\}.dx.b.dz + \int_0^L q.\delta w.dx = 0 \tag{11}$$

The following Eqs. (12-15) are introduced for decoupling of '*x*' and '*z*' parameters.

$$A_{11} = \int_{h/2}^{-h/2} E(z).1.dz \tag{12}$$

$$B_{11} = \int_{h/2}^{-h/2} E(z).z.dz \tag{13}$$

$$D_{11} = \int_{h/2}^{-h/2} E(z).z^2.dz \tag{14}$$

$$K_{55} = \int_{-h/2}^{h/2} k_s.G(z).dz \tag{15}$$

Here 'k_s' is shear correction factor. Substituting the value of ϵ_{xx} followed by simplification and grouping of similar quantities, the following governing equations (Eqs. (16)-(18)) are obtained

$$\frac{\delta U}{\delta u} = A_{11}\frac{\partial^2 u_0}{\partial x^2} + B_{11}\frac{\partial^2 \phi}{\partial x^2} = 0 \tag{16}$$

$$\frac{\delta U}{\delta \phi} = B_{11}\frac{\partial^2 u_0}{\partial x^2} + D_{11}\frac{\partial^2 \phi}{\partial x^2} + K_{55}\left(\phi + \frac{\partial w}{\partial x}\right) = 0 \tag{17}$$

$$\frac{\delta U}{\delta w} = K_{55}\left(\frac{\partial \phi}{\partial x} + \frac{\partial^2 w}{\partial x^2}\right) + q = 0 \tag{18}$$

The following boundary conditions are obtained (Eqs.(19)-(21))

$$N_x = A_{11}\frac{\partial u_0}{\partial x} + B_{11}\frac{\partial \phi}{\partial x} = 0 \tag{19}$$

$$M_x = B_{11}\frac{\partial u_0}{\partial x} + D_{11}\frac{\partial \phi}{\partial x} = 0 \tag{20}$$

$$V_x = K_{55}\left(\phi + \frac{\partial w}{\partial x}\right) = 0 \tag{21}$$

The above equations are governing differential equations and respective boundary conditions for functionally graded beams whose solutions provide an insight to their behavior under different conditions. Eq.(16), when substituted in Eq. (18), eliminates 'u_0'. As the remaining equations are coupled with two parameters, viz. 'w' and 'ϕ', it would be convenient to transform them to a single independent variable, by the following substitutions [26];

$$w = F - \frac{D^*}{K_{55}}\frac{\partial^2 F}{\partial x^2} \tag{22}$$

$$\phi = -\frac{\partial F}{\partial x} \tag{23}$$

After the above substitution, a single fourth order differential equation remains as follows:

$$D^*.\frac{\partial^4 F}{\partial x^4} + q = 0 \tag{24}$$

Using Eq.(22) and (23) the bending moment and shear force will take the form

$$M_x = D^*\frac{\partial^2 F}{\partial x^2} \tag{25}$$

$$V_x = D^*\frac{\partial^3 F}{\partial x^3} \tag{26}$$

As the above equation has been derived from first principles, hence it is valid under all types of environments viz. loading conditions and boundary conditions. Once the independent variable 'F' is determined, the other dependent variables can easily be determined. The solution of Eq. (24) is approached using collocation technique with b-spline basis as approximating functions. The b-spline collocation technique, in the present case uses sixth order b-spline basis functions as approximating polynomials. The governing equation for FG beam (given by Eq.(24)) is fourth order differential equation which is to be solved in its strong form in the present case, unlike the other cases like Galerkin's technique where the order of differential equation is reduced through weak forms. Hence a polynomial of degree 4 or above will be suitable for solving Eq. (24). (Sixth order b-splines are fifth degree polynomials). However with an in view of considering varied cases of material and geometric non-linearity associated with the problem and to explore wider levels of research, higher order of b-spline functions is taken. In order to assess the effect of order of b-spline functions of the approximation accuracy the authors have developed a MATLAB code to incorporate different order for the basis functions.

B-splines are piece-wise polynomials (Fig. 3) made up of linear combinations of b-spline basis functions that can be used to approximate a solution to a mathematical problem. It is drawn in a parametric space 't'. They are defined in terms of order/ degree of the curve and also depend upon a set of non-decreasing coordinates in parametric space which is called a knot-vector. We assume that the knot vector is of open type given by:

$$T = [t_0, t_1, t_2 \ldots\ldots, t_{n+k+1}] \tag{27}$$

where, n+1 = no. of control points and 'k' is order of the polynomial spline. The b-spline basis of 'k^{th}' order is defined recursively using the relation:

$$N_{(i,k)} = \frac{t - t_i}{t_{i+k-1} - t_i} N_{(i,k-1)} + \frac{t_{i+k} - t}{t_{i+k} - t_{i+1}} N_{(i+1,k-1)} \tag{28}$$

In order to use the above relation we need the value of first order basis function, which is defined as follows:

$$N_{i,1} = \begin{cases} 1, t_i < t < t_{i+1} \\ 0, otherwise \end{cases} \tag{29}$$

Using (n+1) control points B_0, B_1... B_n, b-spline function is defined as:

$$B(t) = \sum_{i=0}^{n} N_{i,k}(t).B_i \tag{30}$$

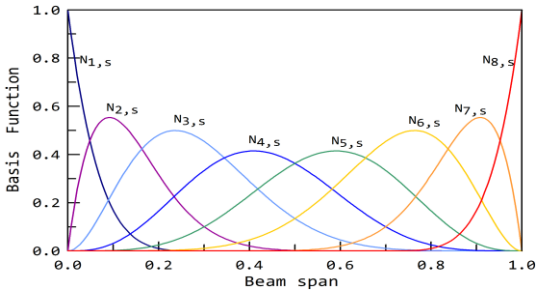

Fig.3
Sixth Order B-spline basis function with non-repeated knots.

The continuity at the intermediate knots is controlled by the multiplicity and is given by the relation C^{k-s-1}, where's' is the multiplicity of the knot. Hence in case of single knots the continuity is C^{k-2}; if the multiplicity is equal to order of the curve (k), then curve becomes discontinuous at that knot. A spline is continuously differentiable up to a limit defined by its order. At a non-repeated knot the spline function is continuous up to (k-2) derivatives, while in case of multiple knots they are differentiable only up to (k-s-1) derivatives. It must be understood here that, in Eq. (24), 'F' is not displacement variable although it has length dimensions. It is simply a quantity that relates the different parameters in such a form that the inter-relationships are largely simplified. 'F' is approximated as;

$$F(t) = \sum_{i=1}^{\mathfrak{N}} F_i N_{i,k}$$

where F_i is a set of control points that define the polygon vertices of b-spline. This leads to $\mathfrak{N}$ unknowns that are to be determined. Let *'m'* be the number of boundary conditions, and hence the number of collocation points required will be $\mathfrak{N}$-m. In this work collocation points are calculated using the method of Greville abscissa [46], defined for a knot vector, $T = [t_0, t_1, t_2 \ldots\ldots, t_{n+k+1}]$ as:

$$x_i = \frac{1}{n}(t_i + t_{i+1} + \ldots + t_{i+n-1}) \tag{31}$$

(where 'n' is the degree of b-spline function and t_i are the knots)

The above leads to $\mathfrak{N}$ values of x_i, the first and the last of which represent the boundaries which have been already used in boundary conditions hence must be omitted. Out of the remaining the points which are located towards center are selected as collocation points. If multiple/ coincident knots are present in the knot vector then it will reduce continuity at that particular knot. In physical space the deflection curve for a beam follows C^2 continuity. A sixth order b-spline function with single knots has a continuity of the order C^4; hence at each junction of spline function the multiplicity of knots must be equal to three. If there are three coincident knots at each junction, then the number of smoothness conditions at point at is also equal to three. This will increase the no. of control points and hence the size of the problem will increase. In order to simplify the procedure we assume (without the loss of generality) that $t_0 = 0$ and $t_{n+k+1}=L$ so as to merge the parametric space with real space; and thereby we may assume $t = x$ [38, 39]. Let the entire length of the beam be divided into *'l'* spans and '*k'* is the order of the approximating spline. Each span is represented by a single spline function as such the total number of spline functions is equal to the no. of spans. As the continuity at the knots equals C^{k-s-1}, the number of smoothness conditions at the knots is (k-s) and hence depends upon the multiplicity*'s'*. Let ϑ_i denote the number of smoothness conditions at each knot. Hence the total no. of coefficients of *'l'* piecewise polynomials or the no. of control points, $\mathfrak{N}$ (n+1) is equal to:

$$\mathfrak{N} = k.l - \sum \vartheta_i \tag{32}$$

The solution of Eq. (24) is approached through b-spline collocation technique and the parameter 'F' is determined. The transverse deflection 'w', slope 'ϕ' are then determined using Eqs. (22)-(23). Substituting Eq. (19) in Eq. (5) and using Eq. (22), the normal and shear stresses are calculated

$$\epsilon_{xx} = \left(-\frac{B_{11}}{A_{11}} + z \right) \frac{\partial \phi}{\partial x} \tag{33}$$

$$\sigma_{xx} = E(z).\epsilon_{xx} = E(z).\left(-\frac{B_{11}}{A_{11}} + z \right) \frac{\partial \phi}{\partial x} \tag{34}$$

$$\sigma_{xx} = E(z).\left(-\frac{B_{11}}{A_{11}} + z \right) \frac{\partial^2 F}{\partial x^2} \tag{35}$$

From the basic elasticity theory we have

$$\frac{\partial \sigma_{xx}}{\partial x} + \frac{\partial \tau_{xz}}{\partial z} = 0 \tag{36}$$

$$\tau_{xz} = \int_{-h/2}^{z} \frac{\partial \sigma_{xx}}{\partial x}.\partial z \tag{37}$$

Substituting Eq. (35) in Eq. (37)

$$\tau_{xz} = \int_{-h/2}^{z} E(z).\left(-\frac{B_{11}}{A_{11}} + z \right) \frac{\partial^3 F}{\partial x^3}.\partial z \tag{38}$$

3 RESULTS AND DISCUSSION

As a numerical example cantilever beam is considered of length L =0.5m, depth h= 0.125m and of unit width. The functionally graded material for the beam is assumed to be a mixture of steel and aluminum, the bottom fibers are steel rich while the top are enriched with aluminum. Their modulus of elasticity are taken as- E_{Steel} = 210 GPa, E_{Al} = 70 GPa. The value of Poisson's ratio is assumed to be a constant and taken as 0.3. The value of power law index is assumed to be equal to 1. An external uniform pressure load applied at the top surface and equal to 1kN is assumed. The beam length is assumed to be divided into three spans of equal length and a sixth order b-spline basis is used in

the collocation process. If we assume non-repeated knots then C^4 continuity at each knot and we have five smoothness conditions at each intermediate knot. The total number of control points from Eq. (32), equals eight. As we have four boundary conditions given by Eq. (1), we need four collocation points as calculated below. Using $k = 6$ and $\mathfrak{N} = 8$ the knot vector is $T = [0\ 0\ 0\ 0\ 0\ 0\ 1/3\ 2/3\ 1\ 1\ 1\ 1\ 1\ 1]$ in normalized form. The collocation points are calculated using Greville abscissa, i.e. Eq. (31):

$$X = [0,\ 0.0667,\ 0.2000,\ 0.4000,\ 0.6000,\ 0.8000,\ 0.9333,\ 1] \tag{39}$$

The X_i (i = 3, 4, 5, 6) are selected as the four collocation points. A MATLAB code is developed to find an approximate solution for Eq. (8) and the value of parameter 'F' is then used to find the transverse displacement 'w', rotation 'ϕ', normal and shear stresses in the beam using the Eq. (22), Eq. (35) and Eq. (38). The calculated values are compared with Reference [26] and are plotted in Fig. 4 (a-c). The verification of results with [26] is also presented in Table 1-2. The above formulation has been extended to study the effect of gradation in material properties on various parameters in a beam. In this regard, deflection or elastic curve for different values of power law index is plotted as shown in Fig. 5 (a-b). In Fig. 5(b), a better insight into the effect of power law index on beam deflection could be ascertained with the help of waterfall plots. It is observed that with the increase in index value the beam becomes stiff. The reason for this is the increase in concentration of steel with high value of stiffness. But the effect is less pronounced as the value of β exceeds 10. The variation of tip deflection with power law index is presented in Table 3. The effect of material gradation on normalized axial stress at three different positions in a beam cross-section viz. top fiber, bottom fiber and at geometrical center are plotted in Fig. 6 (a-c) wherein the effect of power law index on axial stress for functionally graded beams is reported. It is observed that as the value of index increases, induced axial stress decreases which is due to pronounced steel concentration and corresponding behavior. At higher gradation index values (>50), the behavior approaches isotropic. A similar observation from Fig. 6b indicates that at geometrical center the axial stress is not zero and hence neutral axis and geometrical center does not coincide; the higher the index value, lesser is the separation. The behavior reported in Fig. 6(a) and Fig. 6(c) corresponding to different values of β *is* different, i.e. the stress behavior of upper and lower fibers is different. This can be accounted by the fact that with the variation of β the top fiber remains the same i.e. aluminum while the bottom fiber is aluminum for β =0 which changes to steel for β >0. It can be mentioned here that the stress behavior of isotropic material is independent of material property and depends only upon the geometric dimensions. The same is also verified for FG beam with upper and lower materials interchanged. Hence for mid and bottom fiber β =0 must be referred as isotropic case so as to maintain a sequential behavior. The values of maximum normalized stress at different heights of fixed end are given in Table 4., for different power law indices.

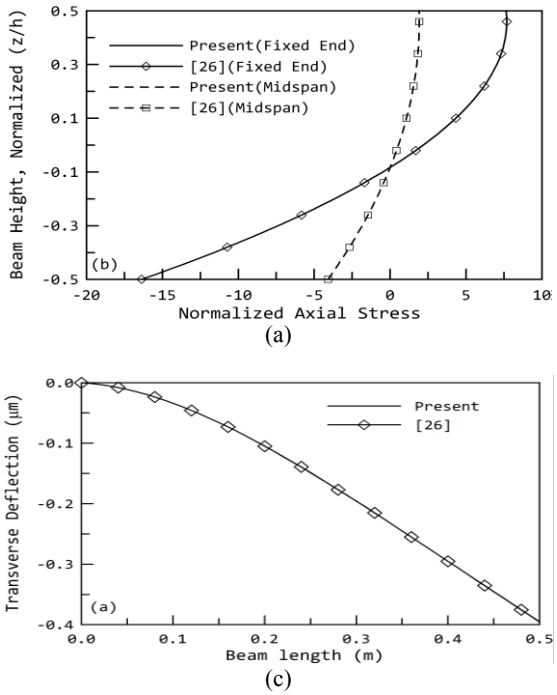

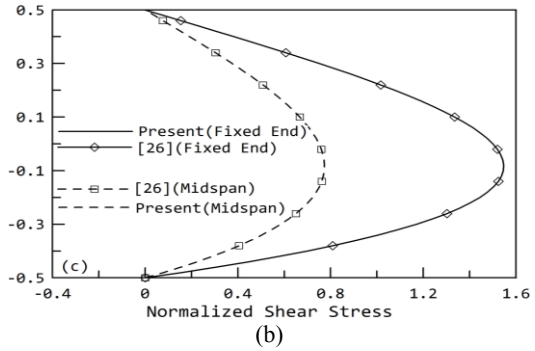

Fig.4
Verification of (a) Beam Deflection, (b) Normalized Axial Stress and (c) Shear Stress with [26].

Table 1
Verification of normalized axial stress with [26].

Normalized Axial Stress						
z/h	(at fixed end)			(at mid-span)		
	Present	Reference 26	% error	Present	Reference 26	% error
-0.5	-16.364	-16.364	1.78E-13	-4.090	-4.090	2.78E-13
-0.4	-11.607	-11.607	1.78E-13	-2.901	-2.901	2.89E-13
-0.3	-7.374	-7.374	2.00E-13	-1.843	-1.843	2.78E-13
-0.2	-3.665	-3.665	2.00E-13	-0.916	-0.916	2.66E-13
-0.1	-0.480	-0.480	1.78E-13	-0.120	-0.120	2.66E-13
0.0	2.181	2.181	1.78E-13	0.545	0.545	2.89E-13
0.1	4.320	4.320	1.78E-13	1.080	1.080	2.89E-13
0.2	5.934	5.934	2.00E-13	1.483	1.483	2.89E-13
0.3	7.025	7.025	2.00E-13	1.756	1.756	2.78E-13
0.4	7.592	7.592	2.00E-13	1.898	1.898	2.66E-13
0.5	7.636	7.636	2.00E-13	1.909	1.909	2.66E-13

Table 2
Verification of normalized shear stress with [26].

Normalized Shear Stress						
z/h	(at fixed end)			(at mid-span)		
	Present	Reference 26	% error	Present	Reference 26	% error
-0.5	-8.92E-17	-8.92E-17	1.02E-12	-4.46E-17	-4.46E-17	3.55E-13
-0.4	0.697	0.697	1.04E-12	0.348	0.348	3.55E-13
-0.3	1.169	1.169	9.99E-13	0.584	0.584	3.77E-13
-0.2	1.443	1.443	1.02E-12	0.721	0.721	3.66E-13
-0.1	1.544	1.544	1.02E-12	0.772	0.772	3.77E-13
0.0	1.500	1.500	1.02E-12	0.750	0.750	3.66E-13
0.1	1.335	1.335	1.02E-12	0.667	0.667	3.44E-13
0.2	1.076	1.076	1.02E-12	0.538	0.538	3.66E-13
0.3	0.750	0.750	1.02E-12	0.375	0.375	3.66E-13
0.4	0.382	0.382	1.02E-12	0.191	0.191	3.44E-13
0.5	-1.78E-16	-1.78E-16	1.02E-12	-8.92E-17	-8.92E-17	3.55E-13

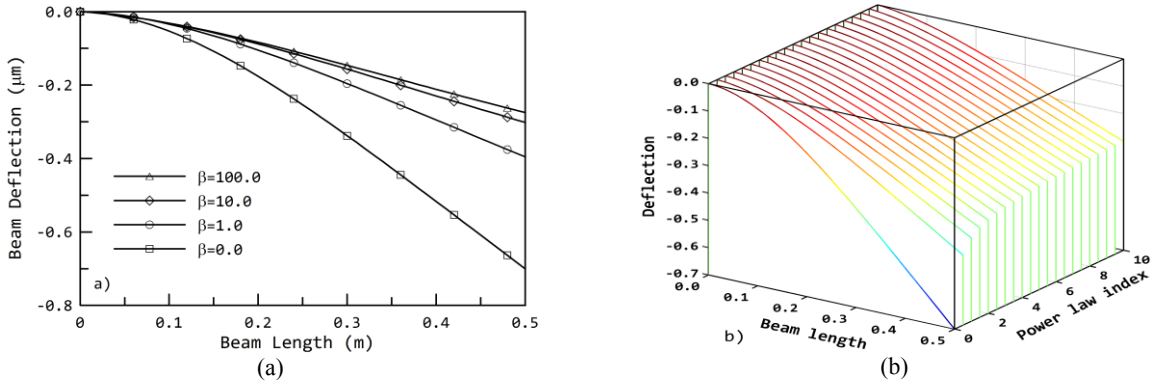

(a) (b)

Fig.5
(a) Beam deflection for different values of β and (b) waterfall plot of deflection with β.

Table 3
Effect of power law index on deflection of free end

Power law index, β	Tip Deflection (μm)	
	Aluminum is at top and steel at bottom	Steel at top and aluminum at bottom
0.0	-0.7000	-0.2710
0.1	-0.5805	-0.2847
0.2	-0.5212	-0.2995
0.5	-0.4430	-0.3423
1.0	-0.3955	-0.3950
2.0	-0.3590	-0.4469
10.0	-0.3016	-0.5290
20.0	-0.2881	-0.5779
50.0	-0.2785	-0.6351
100.0	-0.2751	-0.6640

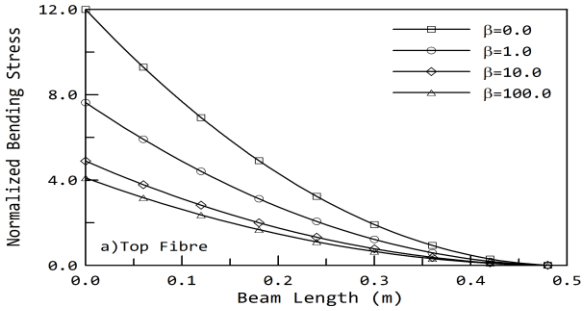

(a)

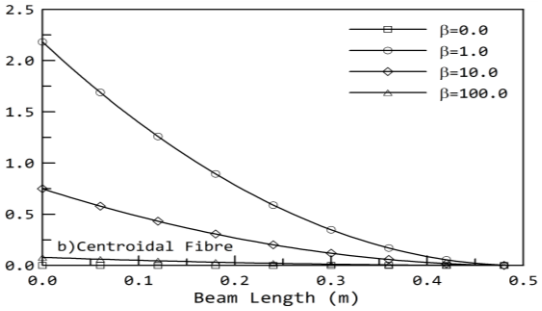

(b)

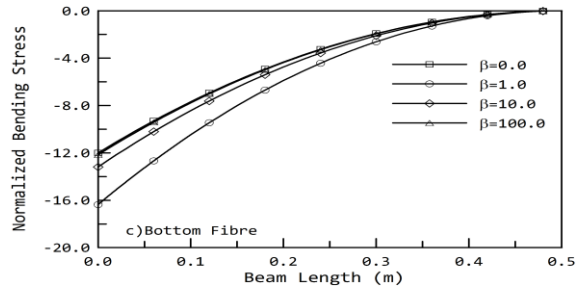

(c)

Fig.6
Plot of normalized axial stress with power law index at (a) Top, (b) Centroidal and (c) Bottom fiber.

Table 4
Variation of normalized axial stress at fixed end with β.

Power law index, β	Maximum value of Normalized Axial stress (i.e. at fixed end)		
	At top fiber	At geometrical centre	At bottom fiber
0.0	12.000	0.000	-12.000
0.1	10.617	0.821	-27.502
0.2	9.844	1.264	-23.506
0.5	8.620	1.885	-18.726
1.0	7.636	2.181	-16.363
2.0	6.666	2.083	-15.000
5.0	5.527	1.330	-13.864
10.0	4.890	0.749	-13.183
20.0	4.487	0.389	-12.682
50.0	4.205	0.158	-12.299
100.0	4.100	0.079	-12.154

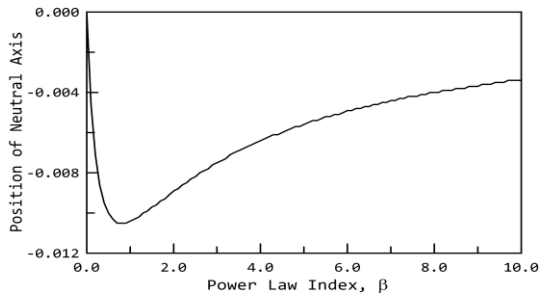

Fig.7
Variation of neutral axis with power law index.

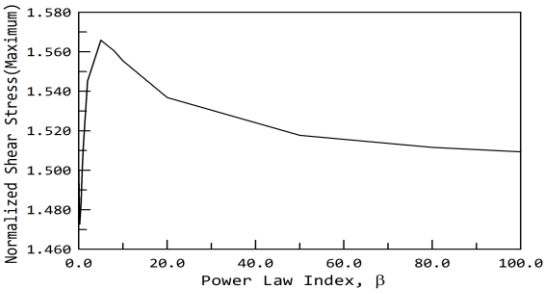

Fig.8
Variation of maximum shear stress with β.

Table 5
Effect of power law index on position of neutral axis.

Power law index, β	Position of neutral axis (*mm*)	
	Aluminum is at top and steel at bottom	Steel at top and aluminum at bottom
0.0	0.0	0.0
0.2	-7.1	3.6
0.4	-9.5	6.1
0.6	-10.3	8.0
0.8	-10.5	9.4
0.9	-10.5	9.9
1.0	-10.4	10.4
1.2	-10.2	11.2
1.4	-9.9	11.7
1.6	-9.6	12.1
1.8	-9.3	12.3
2.0	-8.9	12.5
2.2	-8.6	12.6
2.4	-8.3	12.6
2.6	-8.0	12.6
2.8	-7.8	12.6
3.0	-7.5	12.5

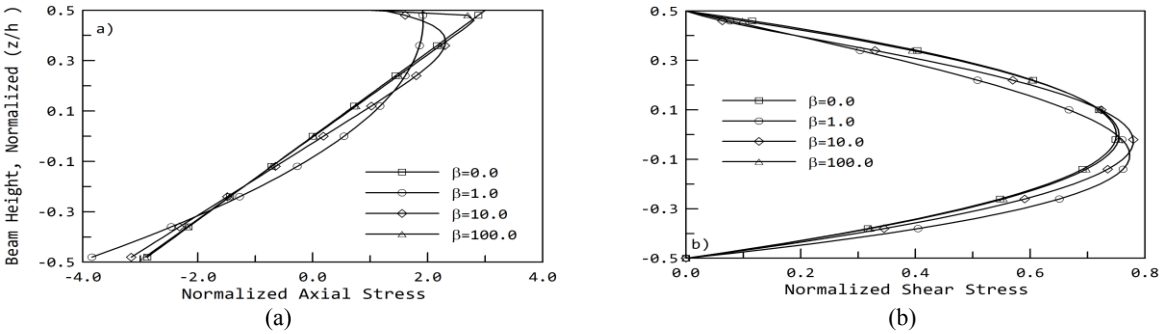

(a) (b)

Fig.9
Variation of normalized axial and shear stress at mid-span along the cross-section with β.

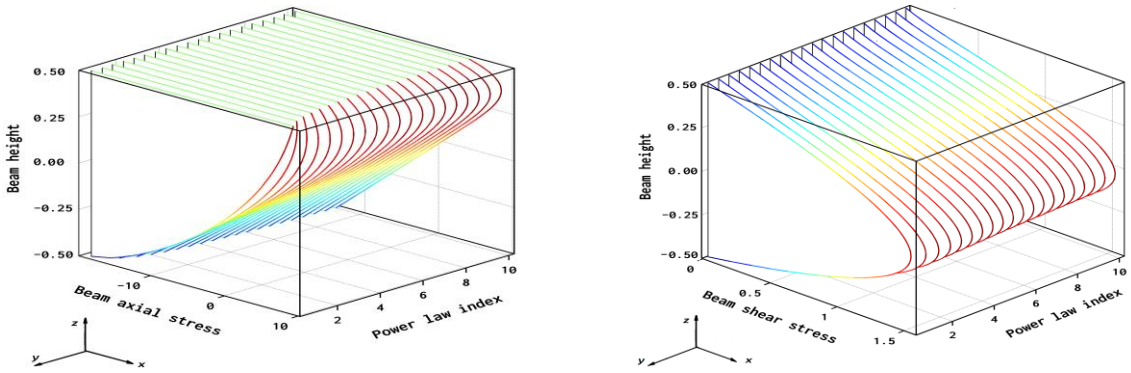

(a) (b)

Fig.10
Waterfall plots of normalized axial and shear stress at fixed end with β.

To study the variation of neutral axis with index value, a plot between the neutral axis positions for different values of β (0 to 10) is shown in Fig. 7 and the values are reported in Table 5. It is observed that as β approaches unity, the neutral axis is located farthest from the centroidal axis of the beam. For β less than unity, the axial stresses at layers below the neutral layer increases till the location of neutral axis from centroidal axis increases. For β greater than unity, the location of neutral layer recedes and asymptotically moves towards the centroidal axis. The axial stresses under such conditions are plotted in Fig. 6(c). The variation of shear stress for shear deformable Timoshenko beam is maximum at the neutral axis. In FG beams the neutral axis do not coincide the geometric center and the maximum shear stress exists at the neutral axis. The variation of maximum normalized shear stress with different values of β is shown in Fig. 8. Variation of normalized axial stress and normalized shear stress along the cross-section for different values of power law index is shown in Fig. 9(a-b) followed by the waterfall plots in Fig. 10(a-b).

4 CONCLUSIONS

A study of cantilever functionally graded Timoshenko beam with grading along the cross-section is reported through this work. The variation of modulus of elasticity and modulus of rigidity is considered by power law and Poisson's ratio is considered to be a constant. The collocation technique using B-spline basis functions is used for solution. The collocation points are calculated using Greville abscissa. Transverse deformation, variation of neutral axis, normalized axial stress and normalized shear stress variations both along the cross-section and along the length of beam of the beam have been plotted with varying power law index values. The following conclusions can be enumerated-

i) The grading plays a considerable role in the deformation and stress characteristics of the beam. With the increase in value of index value the behavior of the beam follows the characteristics of material that is at the bottom.
ii) The stress behavior of top, mid and bottom fibers is quite different. For mid and bottom fiber β =0 must be referred as isotropic case so as to maintain a sequential behavior.
iii) The stress behavior of isotropic material is independent of material property and depends only upon the geometric dimensions.
iv) The neutral axis is observed to shift towards the material with higher elasticity. The neutral axis is at farthest from geometrical center corresponding to index value approaching unity.

REFERENCES

[1] Miyamoto Y., Kaysser W.A., Rabin B.H., Kawasaki A., Ford R.G., 1999, *Functionally Graded Materials, Materials Technology Series*, Springer US, Boston.
[2] Suresh S., Mortensen A., 1998, *Fundamentals of Functionally Graded Materials*, London.
[3] Rasheedat M.M., Akinlabi E.T., 2012, Functionally graded material: An overview, *Proceedings of the World Congress in Engineering*, London, UK.

[4] Udupa G., Rao S.S., Gangadharan K.V., 2014, Functionally graded composite materials: An overview, ***Procedia*** *Materials* ***Science*** **5**: 1291-1299.
[5] Kieback B., Neubrand A., Riedel H., 2003, Processing techniques for functionally graded materials, *Materials Science and Engineering* **362**: 81-106.
[6] Birman V., Byrd L.W., 2007, Modeling and analysis of functionally graded materials and structures, *Applied Mechanics Reviews* **60**: 195.
[7] Reddy J.N., Chin C.D., 1998, Thermomechanical analysis of functionally graded cylinders and plates, *Journal of Thermal Stresses* **21**: 593-626.
[8] Reddy J.N., 2000, Analysis of functionally graded plates, *International Journal for Numerical Methods in Engineering* **47**: 663-684.
[9] Sankar B.V., 2001, An elasticity solution for functionally graded beams, *Composites Science and Technology* **61**: 689-696.
[10] Sankar B.V., Tzeng J.T., 2002, Thermal stresses in functionally graded beams, *AIAA Journal* **40**: 1228-1232.
[11] Zhu H., Sankar B.V., 2004, A combined fourier series–Galerkin method for the analysis of functionally graded beams, *Journal of Applied Mechanics* **71**: 421.
[12] Chakraborty A., Gopalakrishnan S., Reddy J.N., 2003, A new beam finite element for the analysis of functionally graded materials, *International Journal of Mechanical Sciences* **45**: 519-539.
[13] Aydogdu M., Taskin V., 2007, Free vibration analysis of functionally graded beams with simply supported edges, *Materials & Design* **28**: 1651-1656.
[14] Zhong Z., Yu T., 2007, Analytical solution of a cantilever functionally graded beam, *Composites Science and Technology* **67**: 481-488.
[15] Kadoli R., Akhtar K., Ganesan N., 2008, Static analysis of functionally graded beams using higher order shear deformation theory, *Applied Mathematical Modelling* **32**: 2509-2525.
[16] Benatta M.A., Mechab I., Tounsi A., Adda Bedia E.A., 2008, Static analysis of functionally graded short beams including warping and shear deformation effects, *Computational Materials Science* **44**: 765-773.
[17] Sina S.A., Navazi H.M., Haddadpour H., 2009, An analytical method for free vibration analysis of functionally graded beams, *Materials & Design* **30**: 741-747.
[18] Şimşek M., 2010, Fundamental frequency analysis of functionally graded beams by using different higher-order beam theories, *Nuclear Engineering and Design* **240**: 697-705.
[19] Giunta G., Belouettar S., Carrera E., 2010, Analysis of FGM beams by means of classical and advanced theories, *Mechanics of Advanced Materials and Structures* **17**: 622-635.
[20] Tahani M., Torabizadeh M.A., Fereidoon A., 2006, Nonlinear analysis of functionally graded beams, *Journal of Achievements in Materials and Manufacturing Engineering* **18**: 315-318.
[21] Reddy J.N., 2011, Microstructure-dependent couple stress theories of functionally graded beams, *Journal of the Mechanics and Physics of Solids* **59**: 2382-2399.
[22] Zhang D.-G., 2013, Nonlinear bending analysis of FGM beams based on physical neutral surface and high order shear deformation theory, *Composite Structures* **100**: 121-126.
[23] Yaghoobi H., Fereidoon A., 2010, Influence of neutral surface position on deflection of functionally graded beam under uniformly distributed load, *World Applied Sciences Journal* **10**: 337-341.
[24] Mohanty S.C., Dash R.R., Rout T., 2011, Parametric instability of a functionally graded Timoshenko beam on Winkler's elastic foundation, *Nuclear Engineering and Design* **241**: 2698-2715.
[25] Mohanty S.C., Dash R.R., Rout T., 2012, Static and dynamic stability analysis of a functionally graded Timoshenko beam, *International Journal of Structural Stability and Dynamics* **12**: 1250025.
[26] Li X.-F., 2008, A unified approach for analyzing static and dynamic behaviors of functionally graded Timoshenko and Euler–Bernoulli beams, *Journal of Sound and Vibration* **318**: 1210-1229.
[27] Kadalbajoo M.K., Yadaw A.S., 2011, Finite difference, finite element and b-spline collocation methods applied to two parameter singularly perturbed boundary value problems1, *Jnaiam* **5**: 163-180.
[28] Chawla T.C., Leaf G., Chen W., 1975, A collocation method using b-splines for one-dimensional heat or mass-transfer-controlled moving boundary problems, *Nuclear Engineering and Design* **35**: 163-180.
[29] Chawla T.C., Chan S.H., 1979, Solution of radiation-conduction problems with collocation method using b-splines as approximating functions, *International Journal of Heat and Mass Transfer* **22**: 1657-1667.
[30] Bert C.W., Sheu Y., 1996, Static analyses of beams and plates by spline collocation method, *Journal of Engineering Mechanics* **122**: 375-378.
[31] Sun W., 2001, B-spline collocation methods for elasticity problems, *Scientific Computing and Applications* **2001**: 133-141.
[32] Hsu M.-H., 2009, Vibration analysis of non-uniform beams resting on elastic foundations using the spline collocation method, *Tamkang Journal of Science and Engineering* **12**: 113-122.
[33] Hsu M.-H., 2009, Vibration analysis of pre-twisted beams using the spline collocation method, *Journal of Marine Science and Technology* **17**: 106-115.
[34] Wu L.-Y., Chung L.-L., Huang H.-H., 2008, Radial spline collocation method for static analysis of beams, *Applied Mathematics and Computing* **201**: 184-199.

[35] Provatidis C., 2014, Finite element analysis of structures using C 1 -continuous cubic b-splines or equivalent hermite elements, *Journal of Structural* **2014**: 1-9.
[36] Cottrell J.A., Hughes T.J.R., Bazilevs Y., 2009, *Isogeometric Analysis: Toward Integration of CAD and FEA*, Wiley, Chichester.
[37] Auricchio F., Da Veiga L.B., Hughes T.J.R., Reali A., Sangalli G., 2010, Isogeometric collocation methods, *Mathematical Models and Methods in Applied Sciences* **20**: 2075-2107.
[38] Reali A., Gomez H., 2015, An isogeometric collocation approach for Bernoulli–Euler beams and Kirchhoff plates, *Computer Methods in Applied Mechanics and Engineering* **284**: 623-636.
[39] Patlashenko I., 1993, Cubic b-spline collocation method for non-linear static analysis of panels under mechanical and thermal loadings, *Computers & Structures* **49**: 89-96.
[40] Patlashenko I., Weller T., 1995, Two dimensional spline collocation method for nonlinear analysis of laminated panels, *Computers & Structures* **57**: 131-139.
[41] Mizusawa T., Kito H., 1995,Vibration of cross ply laminated cylindrical panels by spline strip method, *Computers & Structures* **57**: 253-267.
[42] Mizusawa T., 1996, Vibration of thick laminated cylindrical panels by spline strip method, *Computers & Structures* **61**: 441-457.
[43] Akhras G., Li W., 2011, Stability and free vibration analysis of thick piezoelectric composite plates using finite strip method, *Journal of Mechanical Sciences* **53**: 575-584.
[44] Loja M.A.R., Mota Soares C.M., Barbosa J.I., 2013, Analysis of functionally graded sandwich plate structures with piezoelectric skins, using b-spline finite strip method, *Computers & Structures* 96: 606-615.
[45] Provatidis C.G., 2017, B-splines collocation for plate bending eigen analysis, *Journal of Mechanics of Materials and Structures* **12**: 353-371.
[46] Johnson R.W., 2005, Higher order b-spline collocation at the Greville abscissae, *Applied Numerical Mathematics* **52**: 63-75.